

# A submillisecond-response liquid crystal for color sequential projection displays

Fenglin Peng  
Fangwang Gou  
Haiwei Chen  
Yuge Huang  
Shin-Tson Wu

**Abstract** — We report a new LC with low viscosity and high clearing point ( $T_c \sim 102^\circ\text{C}$ ) for color-sequential projection displays. Using a  $1.95\text{-}\mu\text{m}$  mixed-mode twisted nematic cell, the averaged gray-to-gray response time is less than 1 ms, which is  $\sim 3.6\times$  faster than the current state of the art. Such a mixed-mode twisted nematic liquid-crystal-on-silicon can be used for near-to-eye wearable projection displays and head-up displays in vehicles.

**Keywords** — *submillisecond-response, projection, color sequential, liquid-crystal-on-silicon (LCoS).*

DOI # 10.1002/jsid.434

## 1 Introduction

Field sequential color liquid-crystal-on-silicon (LCoS) has been widely used in projection displays, wearable displays, and head-up displays in vehicles.<sup>1,2</sup> By eliminating the color filters, both resolution density and optical efficiency are tripled. However, it requires fast response time (e.g.,  $<1$  ms) to suppress color breakup and keep high image quality. To achieve sub-millisecond response time, several approaches have been investigated such as (1) employing fast response liquid crystal mode like ferroelectric liquid crystal<sup>3</sup> and polymer-stabilized blue phase liquid crystal.<sup>4</sup> However, high operation voltage and low reflectance still remain to be overcome before widespread applications can be realized. (2) Using a thin vertical alignment liquid crystal cell.<sup>5</sup> Though it exhibits high contrast ratio, the fringing field effect degrades the reflectance, especially in a high-resolution panel.<sup>6</sup> On the other hand, mixed-mode twist nematic (MTN)<sup>7</sup> shows several advantages for reflective LCoS projection displays, such as high reflectance, low operation voltage, and weak fringing field effect. Its response time is proportional to  $d^2$  and visco-elastic coefficient ( $\gamma_1/K_{11}$ ). To speed up the response time of MTN mode, two approaches are considered: (1) using a thin cell gap ( $d$ ), which requires a large birefringence ( $\Delta n$ ) LC to achieve high reflectance; and (2) employing a low viscosity LC mixture.<sup>8</sup> Because of thermal effect from the employed high power arc lamp or LED, the LCoS panel temperature could rise to  $\sim 35\text{--}55^\circ\text{C}$ . For head-up displays inside a car, the operation temperature could easily exceed  $80^\circ\text{C}$  during summer time, depending on the geographic location.<sup>9</sup> This imposes a stringent requirement on the high clearing point ( $T_c$ ) of the LC candidates. To achieve high  $T_c$ , some three-ring and four-ring compounds are commonly used, which would dramatically increase the viscosity and lengthen the response time.

In this paper, we report a new LC mixture with high clearing point ( $T_c \sim 102^\circ\text{C}$ ) and low viscosity. Besides, it exhibits a modest  $\Delta n$  and positive dielectric anisotropy ( $+\Delta\epsilon$ ). The physical properties are measured at different temperatures. Employing the measured material parameters in a MTN LCoS, we find the average gray-to-gray (GTG) rise time is 0.5 ms and decay time is 0.2 ms at  $T = 55^\circ\text{C}$ . At  $T = 35^\circ\text{C}$ , the corresponding GTG rise time is 1.0 ms and decay time is 0.4 ms. Promising applications for head-up vehicular displays and near-to-eye wearable projection displays are foreseeable.

## 2 Experiment and results

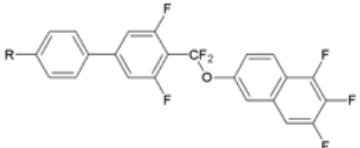
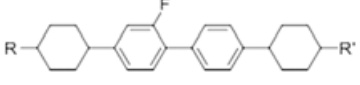
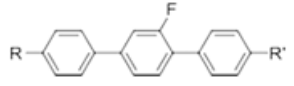
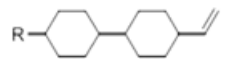
In experiment, we collaborated with DIC (Japan) and prepared a LC mixture, designated as DIC-57F-15. Table 1 lists the chemical structures of major compounds used in the LC mixture. The homologues (different alkyl chain length R) of Compound 1 exhibits high birefringence ( $\Delta n \sim 0.20$ ) and large dielectric anisotropy ( $\Delta\epsilon \sim 30$ ).<sup>10</sup> The three-ring and four-ring compounds (Compounds 2 and 3) are added to further increase the clearing point while maintaining a high  $\Delta n$ . In addition, we also doped  $\sim 50$  wt % non-polar diluters (i.e., Compound 4) to reduce the viscosity and activation energy. We used differential scanning calorimetry (TA Instrument Q100) to measure the phase transition temperatures. The melting point is below  $-40^\circ\text{C}$  (limited by our differential scanning calorimetry), and the clearing point is  $102^\circ\text{C}$ . To determine the dielectric anisotropy, we measured the capacitance of a homogeneous cell and a homeotropic cell using an HP-4274 multi-frequency LCR meter, and the measured results are  $\Delta\epsilon = 5.0$  at  $25^\circ\text{C}$  and 4.7 at  $55^\circ\text{C}$ .

Received 02/15/16; accepted 03/08/16.

The authors are with the College of Optics and Photonics, University of Central Florida, Orlando, FL 32816, USA; e-mail: swu@creol.ucf.edu.

© Copyright 2016 Society for Information Display 1071-0922/16/2404-0434\$1.00.

**TABLE 1** — Chemical structures and major compositions of DIC-57 F-15.

No.	Chemical structures	wt %
1		~20
2		~10
3		~20
4		~50

## 2.1 Birefringence

Birefringence was measured through phase retardation of a homogeneous cell sandwiched between two crossed polarizers.<sup>11</sup> The cell gap was controlled at  $\sim 5.05 \mu\text{m}$  by spacers. The indium tin oxide glass substrates were overcoated with a thin polyimide (PI) layer rubbed in anti-parallel directions to create  $2^\circ$  pre-tilt angle and strong anchoring energy. We put the LC cell in a Linkam LTS 350 Large Area Heating/Freezing Stage controlled by TMS94 Temperature Programmer and applied a 1 kHz square-wave AC voltage signal. The light sources are a tunable Argon-ion laser ( $\lambda = 457, 488, \text{ and } 514 \text{ nm}$ ) and a He-Ne laser ( $\lambda = 633 \text{ nm}$ ). The transmitted light was measured by a photodiode and recorded by a LabVIEW data acquisition system. The birefringence was measured from  $0\text{--}80^\circ\text{C}$  at  $\lambda = 633 \text{ nm}$  as shown in Fig. 1(a). Black squares stand for the measured data, and the red line is the fitting curve using Haller's semi-empirical equation:<sup>12</sup>

$$\Delta n = \Delta n_0(1 - T/T_c)^\beta, \quad (1)$$

where  $n_0$  is the extrapolated birefringence at  $T = 0 \text{ K}$  and  $\beta$  is a material constant.  $S = (1 - T/T_c)^\beta$  is the order parameter. From the fitting, we found that  $n_0 = 0.15$  and  $\beta = 0.16$ .

To investigate the electro-optic performance at different wavelengths, we also measured the dispersion curve at  $25^\circ\text{C}$ . The results are shown in Fig. 1(b). Black squares represent the measured data and the solid line is the fitting result with single-band birefringence dispersion model:<sup>13</sup>

$$\Delta n = G \frac{\lambda^2 \lambda^{*2}}{\lambda^2 - \lambda^{*2}}. \quad (2)$$

Here,  $G$  is a proportionality constant and  $\lambda^*$  is the mean resonance wavelength. Through fitting, we obtained  $G = 1.867 \mu\text{m}^{-2}$  and  $\lambda^* = 0.232 \mu\text{m}$ . In principle,  $n_0$  should also follow the single-band dispersion model but at a different  $G$  (denoted as  $G_0$ ). From these two equations and the fitted parameters, birefringence at other wavelengths can be deduced at a specified temperature. We obtained that at  $T = 55^\circ\text{C}$ ,  $\Delta n = 0.105, 0.112, \text{ and } 0.125$  at  $\lambda = 450, 550, \text{ and } 650 \text{ nm}$ ; these data will be used in the simulation later.

## 2.2 Visco-elastic coefficient

From the response time measurement, we extracted the visco-elastic coefficient ( $\gamma_1/K_{11}$ ) at different temperatures, as shown in Fig. 2. The black squares and the red solid line represent the measured data and fitting curve, respectively. The fitting equation is expressed as follows:<sup>14</sup>

$$\frac{\gamma_1}{K_{11}} = A \frac{\exp(E_a/k_B T)}{(1 - T/T_c)^\beta}. \quad (3)$$

In Eq. 3,  $A$  is a proportionality constant,  $k_B$  is the Boltzmann constant, and  $E_a$  is the activation energy.  $\beta$  is the

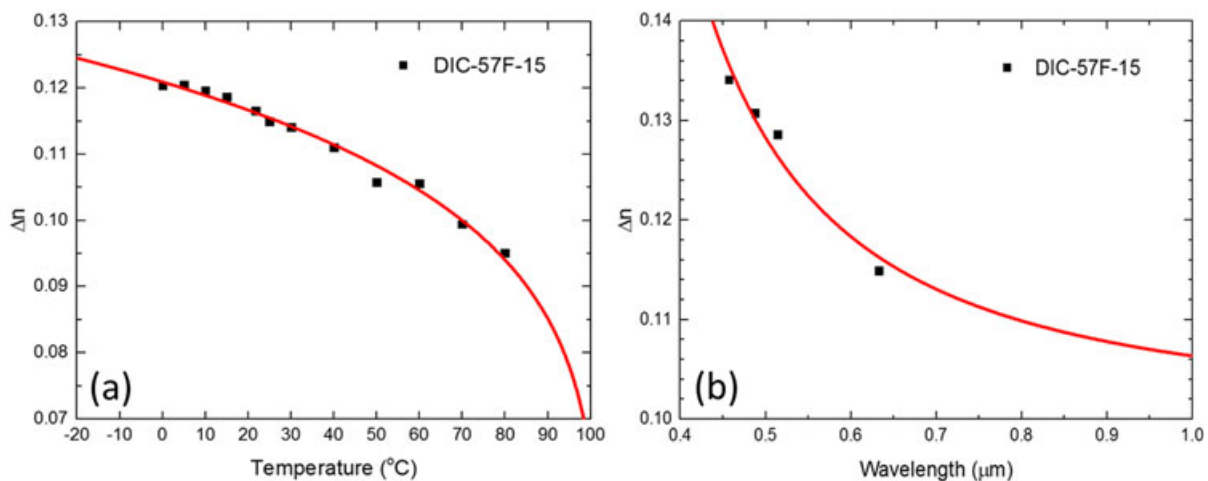


**FIGURE 1** — (a) Temperature dependent birefringence curve at  $\lambda = 633 \text{ nm}$ ; (b) birefringence dispersion curve at  $T = 25^\circ\text{C}$ .

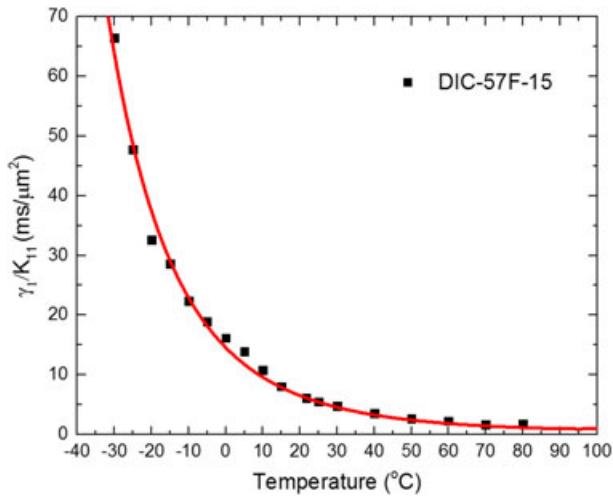


FIGURE 2 — Temperature dependent  $\gamma_1/K_{11}$  of DIC-57 F-15. Dots are experimental data and solid line is fitting with Eq. 3.

material constant, which has been obtained from Eq. 1. Through fitting, we obtained  $E_a = 290$  meV. Based on the fitting curve, we found that  $\gamma_1/K_{11} = 2.10$  ms/ $\mu\text{m}^2$  at  $T = 55^\circ\text{C}$ , which is less than half of that at room temperature.

### 2.3 Long-term stability

For wearable display at outdoor or head-up display in a vehicle, the LCD panel could be exposed to sunlight or high temperature during summer time. Therefore, long-term stability of liquid crystal mixture at warm environment is another concern. In an LCD panel, the employed polarizers and indium tin oxide-glass substrates help to filter out the short-wavelength UV light because of the inherent absorption. To perform accelerated reliability test, we put a bottle of DIC-57F-15 and a filled LC cell in an oven, whose temperature was controlled at  $T = 85^\circ\text{C}$  for 12 days. We took out the LC cell (and LC bottle) and measured its birefringence ( $\Delta n$ ) at  $T = 25^\circ\text{C}$  (and clearing point) every day. Figure 3 shows the measured results during this period. The variation of

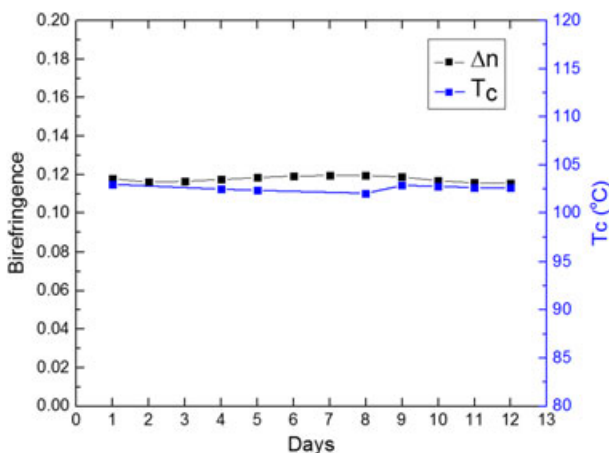


FIGURE 3 — Birefringence and clearing point stability of DIC-57 F-15. The storage temperature is controlled at  $T = 85^\circ\text{C}$ .

birefringence is  $\sim 3\%$ , and the clearing point is less than 1%, which indicates our LC material and LC cell exhibit an excellent stability under high temperature environment. For a high-brightness LCoS projector using LED light sources, there is no UV component. The only harmful UV content comes from ambient light. Our LC structures consist of no conjugated double or triple bonds. As a result, their UV stability is superb. The only weak part is polyimide alignment layer. Therefore, for high-brightness LCoS applications, we should replace the organic polyimide with inorganic alignment layers, such as  $\text{SiO}_x$ .<sup>15</sup>

## 3 Electro-optic performance of mixed-mode twisted nematic liquid-crystal-on-silicon

We used a commercial LCD simulator DIMOS 2.0 to calculate the electro-optic properties of a MTN LCoS. The LC directors are twisted by  $90^\circ$  from top to bottom substrates (i.e., MTN  $90^\circ$ ). In addition, other parameters were set as  $d = 1.95$   $\mu\text{m}$ ,  $\Delta n = 0.112$  at  $\lambda = 550$  nm, and  $\gamma_1/K_{11} = 2.10$  ms/ $\mu\text{m}^2$  at  $T = 55^\circ\text{C}$ . The angle between front LC directors and the polarizing beam splitter polarization axis is set at  $20^\circ$  to maximize the reflectance, and the initial pretilt angle is  $\sim 2^\circ$ . MTN- $90^\circ$  modulates the light reflectance through both polarization rotation and phase retardation effects. A reflector is placed on the inner surface of the MTN- $90^\circ$  cell. For the blue and red beams, we used  $\Delta n = 0.112$  and  $0.105$ , respectively, to take birefringence dispersion into consideration. The voltage-dependent reflectance (VR) curves for the RGB colors are shown in Fig. 4. A common good dark state is obtained at 4.5V. Thus, only a single gamma curve is needed for driving the RGB frames.

To calculate the GTG response time, we divided the VR curve at  $\lambda = 550$  nm into eight gray levels. The results are summarized in Table 2. Both rise time and decay time are

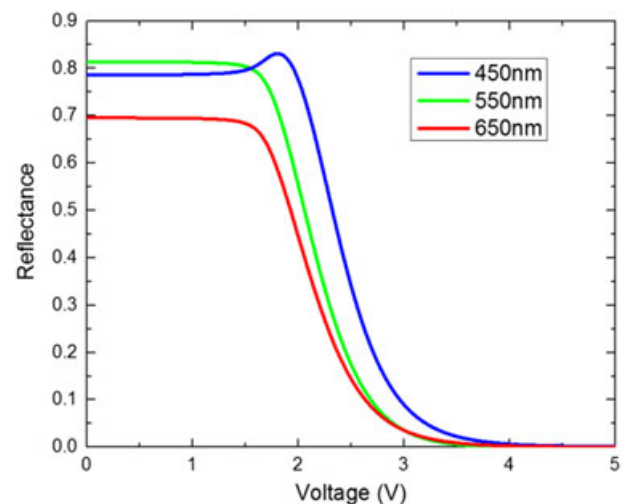


FIGURE 4 — Simulated voltage-dependent reflectance curves at the specified RGB colors. Cell gap  $d = 1.95$   $\mu\text{m}$ .

**TABLE 2** — Calculated GTG response time (ms) of the MTN cell for DIC-57 F-15.

	1	2	3	4	5	6	7	8
1		0.23	0.30	0.37	0.46	0.56	0.71	1.00
2	0.25		0.13	0.24	0.35	0.47	0.64	0.97
3	0.29	0.08		0.12	0.23	0.37	0.55	0.94
4	0.30	0.13	0.06		0.13	0.27	0.47	0.91
5	0.31	0.17	0.10	0.05		0.15	0.36	0.90
6	0.33	0.21	0.15	0.10	0.05		0.23	0.89
7	0.36	0.25	0.20	0.15	0.11	0.07		0.92
8	0.43	0.34	0.29	0.26	0.24	0.22	0.20	

defined as 10–90% reflectance change. By applying overdrive and undershoot voltages,<sup>16</sup> we obtained average GTG rise time of 0.50 ms and decay time 0.20 ms. Such a fast response time helps to mitigate the color breakup of the color sequential LCoS projection display. For projection displays using LED light sources, the chassis temperature is around 35 °C. Based on Fig. 2, the extrapolated GTG rise time is 1.0 ms and decay time 0.40 ms, which are still quite fast.

In a color-filter-embedded LCoS display,<sup>17</sup> the applied voltage is partially shielded by the color filters. As a result, the effective voltage the LC layer experiences is lower than the applied voltage because of limited storage capacitance and voltage shielding effect.<sup>18</sup> Therefore, an LC mixture with slightly higher dielectric anisotropy ( $\Delta\epsilon \sim 8\text{--}10$ ) would help lower the on-state voltage, which in turn leads to a higher contrast ratio. However, as the dielectric anisotropy increases, the rotational viscosity of the LC increases linearly, assuming the  $T_c$  and  $\Delta n$  remain approximately the same.<sup>19</sup> Therefore, employing LCs with a larger  $\Delta\epsilon$  helps to reduce operation voltage and increase contrast ratio, but the tradeoff is slower response time, especially at low temperatures.

## 4 Conclusion

A high performance LC mixture with high  $T_c$ , low viscosity, modest  $\Delta n$  and  $\Delta\epsilon$ , excellent long-term stability is reported. This mixture is developed by DIC and will be commercially available soon. Using the LC mixture, the MTN LCoS shows sub-millisecond response time at an elevated temperature, which enables color sequential projection display with negligible color breakup and suppressed fringing field effects. By eliminating the spatial color filters, both resolution density and optical efficiency are tripled. As a result, this device can be used for near-to-eye wearable projection displays and head-up displays in vehicles.

## Acknowledgments

The authors are indebted to DIC Corporation, Japan, for providing LC mixtures, and Air Force Office of Scientific Research (AFOSR) for partial financial supports under contract No. FA9550-14-1-0279.

## References

- 1 E. H. Stupp and M. S. Brennessoltz, *Projection Displays*. John Wiley & Sons Inc., (1999).
- 2 K. H. Fan-Chiang *et al.*, “LCoS panel using novel color sequential technology,” *SID Int. Symp. Digest Tech. Papers*, **38**, No. 1, 150–153 (2007).
- 3 V. Chigrinov, “Fast high resolution ferroelectric liquid crystal displays,” *SID Int. Symp. Digest Tech. Papers*, **45**, No. 1, 90–92 (2014).
- 4 L. Rao, S. He and S. T. Wu, “Blue-phase liquid crystals for reflective projection displays,” *J. Display Technol.*, **8**, No. 10, 555–558 (2012).
- 5 Y. Chen, F. Peng and S. T. Wu, “Submillisecond-response vertical-aligned liquid crystal for color sequential projection displays,” *J. Display Technol.*, **9**, No. 2, 78–81 (2013).
- 6 K. H. Fan-Chiang *et al.*, “Fringing-field effects on high-resolution liquid crystal microdisplays,” *J. Display Technol.*, **1**, No. 2, 304 (2005).
- 7 S. T. Wu and C. S. Wu, “Mixed-mode twisted nematic liquid crystal cells for reflective displays,” *Appl. Phys. Lett.*, **68**, No. 11, 1455–1457 (1996).
- 8 H. Chen *et al.*, “Ultra-low viscosity liquid crystal materials,” *Opt. Mater. Express*, **5**, No. 3, 655–660 (2015).
- 9 M. Schadt *et al.*, “New liquid crystal materials; physical properties and performance in displays for automobile, high information density and guest-host applications,” *Mol. Cryst. Liq. Cryst.*, **94**, No. 1–2, 139–153 (1983).
- 10 H. Takatsu, *Advanced liquid crystal materials for active matrix displays*, Conf. Proc. *Advanced Display Materials and Devices*, p.43 (2014).
- 11 S. T. Wu, U. Efron and L. D. Hess, “Birefringence measurements of liquid crystals,” *Appl. Opt.*, **23**, No. 21, 3911–3915 (1984).
- 12 I. Haller, “Thermodynamic and static properties of liquid crystals,” *Prog. Solid State Chem.*, **10**, 103–118 (1975).
- 13 S. T. Wu, “Birefringence dispersions of liquid crystals,” *Phys. Rev. A*, **33**, No. 2, 1270–1274 (1986).
- 14 S. T. Wu, A. M. Lackner and U. Efron, “Optimal operation temperature of liquid crystal modulators,” *Appl. Opt.*, **26**, No. 16, 3441–3445 (1987).
- 15 C. H. Wen *et al.*, “Photostability of liquid crystals and alignment layers,” *J. Soc. Info. Display*, **13**, No. 9, 805–811 (2005).
- 16 S. T. Wu, “Nematic liquid crystal modulator with response time less than 100  $\mu\text{s}$  at room temperature,” *Appl. Phys. Lett.*, **57**, No. 10, 986–988 (1990).
- 17 Y. W. Li *et al.*, “LCoS using a fringe-field color filter,” *SID Int. Symp. Digest Tech. Papers*, **43**, No. 1, 914–917 (2012).
- 18 M. Jiao *et al.*, “Alignment layer effects on thin liquid crystal cells,” *Appl. Phys. Lett.*, **92**, 061102 (2008).
- 19 F. Peng *et al.*, “High performance liquid crystals for vehicle displays,” *Opt. Mater. Express*, **6**, No. 3, 717–726 (2016).



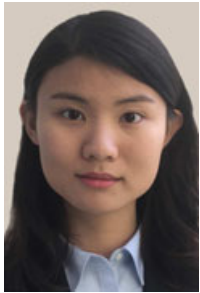
**Fenglin Peng** received her B.S. degree from Zhejiang University, China in 2012. She is currently a PhD candidate at College of Optics and Photonics, University of Central Florida, USA. Her research interests include novel liquid crystal materials development and devices design for display and photonics applications. She has published 20 journal papers and received SID Distinguished Student Paper Awards three times.



**Fangwang Gou** received her B.S. degree from University of Electronic and Science and Technology of China in 2012 and M.S. degree from Peking University, China, in 2015. Currently, she is working toward the PhD degree at College of Optics and Photonics, University of Central Florida, USA. Her current research interests include liquid crystal materials and devices for display and photonic applications.



**Haiwei Chen** received his B.S. degree in optoelectronic information engineering from Beihang University, Beijing, China, in 2013 and is currently working toward the PhD degree at College of Optics and Photonics, University of Central Florida, Orlando, FL, USA. His research focuses on wide color gamut, high dynamic range, and fast-response liquid crystal display devices. He received SID Distinguished Student Paper Award in 2015. Presently, he is president of SID student chapter at UCF.



**Yuge Huang** received her B.S. degree in Physics from Nanjing University, China, in 2015. Currently, she is working toward the PhD degree at College of Optics and Photonics, University of Central Florida, USA. Her research focuses include polymer-stabilized blue phase liquid crystals and polymer network liquid crystals for display and photonic applications.



**Shin-Tson Wu** is Pegasus professor at College of Optics and Photonics, University of Central Florida. He is among the first six inductees of the Florida Inventors Hall of Fame (2014) and a Charter Fellow of the National Academy of Inventors (2012). He is a Fellow of the IEEE, OSA, SID, and SPIE, and the recipient of 2014 OSA Esther Hoffman Beller medal, 2011 SID Slottow-Owaki prize, 2010 OSA Joseph Fraunhofer award, 2008 SPIE G. G. Stokes award, and 2008 SID Jan Rajchman prize. Presently, he is serving as SID honors and awards committee chair and SPIE G. G. Stokes award committee member.